RESEARCH ARTICLE

Electroacupuncture modulates the activity of the hippocampus-nucleus tractus solitarius-vagus nerve pathway to reduce myocardial ischemic injury

Shuai Cui[1, 2], Kun Wang[1], Sheng-Bing Wu[3], Guo-Qi Zhu[3], Jian Cao[4], Yi-Ping Zhou[1], Mei-Qi Zhou[1, 3, *]

1 Research Institute of Acupuncture and Meridian, Anhui University of Chinese Medicine, Hefei, Anhui Province, China

2 Clinical Medical College of Acupuncture, Moxibustion and Rehabilitation, Guangzhou University of Chinese Medicine, Guangzhou, Guangdong Province, China

3 Key Laboratory of Xin' An Medicine, Ministry of Education, Anhui University of Chinese Medicine, Hefei, Anhui Province, China

4 Department of Science and Technology, Anhui University of Chinese Medicine, Hefei, Anhui Province, China

Funding: *This study was supported by the National Natural Science Foundation of China, No. 81273858; a grant from the Anhui University Research and Innovation Platform Team Construction Project in China, No. 2015TD033.*

Graphical Abstract

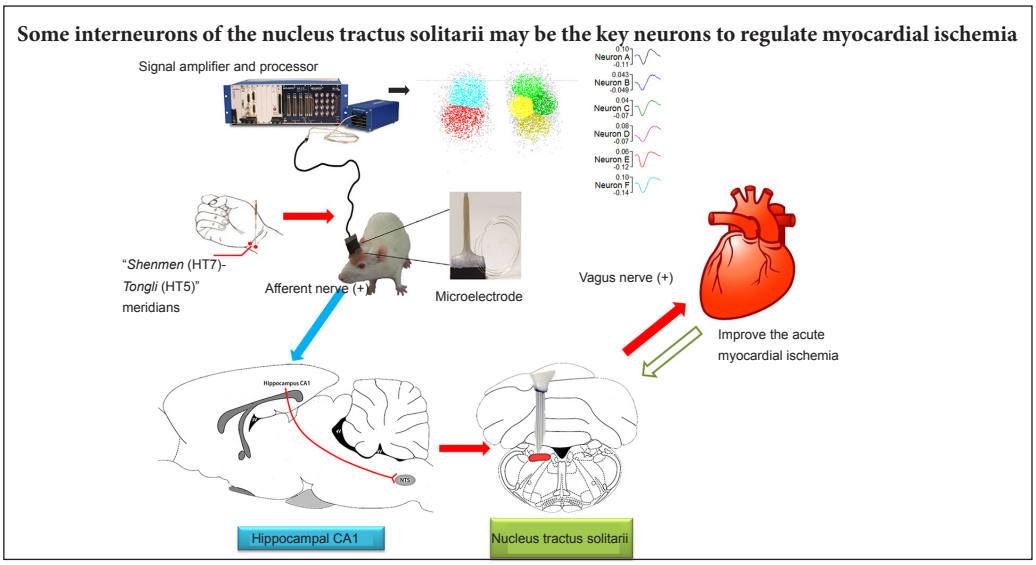

Correspondence to:
Mei-Qi Zhou, Ph.D., meiqizhou@163.com.

orcid:
0000-0002-1728-4252 (Mei-Qi Zhou)

doi: *10.4103/1673-5374.237124*

Accepted: *2018-06-12*

Abstract

The hippocampus is involved in the regulation of the autonomic nervous system, together with the hypothalamus and brainstem nuclei, such as the paraventricular nucleus and nucleus tractus solitarius. The vagus nerve-nucleus tractus solitarius pathway has an important role in cardiovascular reflex regulation. Myocardial ischemia has been shown to cause changes in the autonomic nervous system, affecting the dynamic equilibrium of the sympathetic and vagal nerves. However, it remains poorly understood how the hippocampus communicates with brainstem nuclei to regulate the autonomic nervous system and alleviate myocardial ischemic tissue damage. A rat model of acute myocardial ischemia (AMI) was made by ligating the left anterior descending branch of the coronary artery. Three days before ischemia, the hippocampal CA1 region was damaged. Then, 3 days after ischemia, electroacupuncture (EA) at *Shenmen* (HT7)-*Tongli* (HT5) was performed (continuous wave, 1 mA, 2 Hz, duration of 30 minutes). Cluster analysis of firing patterns showed that one type of neuron was found in rats in the sham and AMI groups. Three types of neurons were observed in the AMI + EA group. Six types of neurons were found in the AMI + EA + Lesion group. Correlation analysis showed that the frequency of vagus nerve discharge in each group was negatively correlated with heart rate (HR) ($P < 0.05$, $r = -0.424$), and positively correlated with mean arterial pressure (MAP) ($P < 0.05$, $r = 0.40987$) and the rate-pressure product (RPP) ($P < 0.05$, $r = 0.4252$). The total frequency of the nucleus tractus solitarius discharge in each group was positively correlated with vagus nerve discharge ($P < 0.01$, $r = 0.7021$), but not with hemodynamic index (HR: $P > 0.05$, $r = -0.03263$; MAP: $P > 0.05$, $r = -0.08993$; RPP: $P > 0.05$, $r = -0.03263$). Some neurons (Neuron C) were negatively correlated with vagus nerve discharge, HR, MAP and RPP in the AMI + EA group (vagus nerve discharge: $P < 0.05$, $r = -0.87749$; HR: $P < 0.01$, $r = -0.91902$; MAP: $P < 0.05$, $r = -0.85691$; RPP: $P < 0.01$, $r = -0.91902$). Some neurons (Neurons C, D and E) were positively correlated with vagus nerve discharge, HR, MAP and RPP in the AMI + EA + Lesion group (vagus nerve discharge: $P < 0.01$, $r = 0.8905$, $P < 0.01$, $r = 0.9725$, $P < 0.01$, $r = 0.9054$; HR: $P < 0.01$, $r = 0.9347$, $P < 0.01$, $r = 0.9089$, $P < 0.05$, $r = 0.8247$; MAP: $P < 0.05$, $r = 0.8474$, $P < 0.01$, $r = 0.9691$, $P < 0.01$, $r = 0.9027$; RPP: $P < 0.05$, $r = 0.8637$, $P < 0.01$, $r = 0.9407$, $P < 0.01$, $r = 0.9027$). These findings show that the hippocampus-nucleus tractus solitarius-vagus nerve pathway is involved in the cardioprotective effect of EA at the heart meridian. Some interneurons in the nucleus tractus solitarius may play a particularly important role in the cardiomodulatory process.

Key Words: *nerve regeneration; acute myocardial ischemia; hippocampus; nucleus tractus solitarius; vagus nerve discharge; electroacupuncture; Shenmen (HT7); Tongli (HT5); autonomic nerve; neural regeneration*

Introduction

Acute myocardial ischemia (AMI) can be caused by a reduction in blood supply or blockage of the coronary artery. This leads to severe acute ischemia in myocardial tissue, resulting in myocardial ischemic necrosis (Lu and Zhong, 2009; Chen et al., 2016). The World Health Organization in 2004 reported on the global burden of 136 diseases, and showed that ischemic heart disease is the leading cause of death, accounting for 12.2% of all deaths. That number is expected to rise to 14.2% by 2030. Myocardial ischemia is associated with sudden cardiac death (Zaman and Kovoor, 2014) and high disability and mortality, and is a major focus of cardiovascular disease research.

The hippocampus is involved in regulating the autonomic nervous system by the endocrine system, together with the hypothalamus and brainstem nuclei, including the paraventricular nucleus and nucleus tractus solitarius (NTS) (Liu et al., 2007). A previous study showed that myocardial ischemia increases expression of the N-methyl-D-aspartic acid receptor NR1 and NR2B subunits in the rat hippocampus, thereby activating this brain region (Zhu et al., 2012). Myocardial ischemia can also cause cognitive dysfunction in the hippocampus. For example, transient changes in cognitive function after acute myocardial ischemia/reperfusion injury is associated with an increase in tumor necrosis factor alpha and interleukin-1 beta mRNA and protein expression in the hippocampus (Zhu et al., 2008). The NTS is the primary reflex center of the viscera, and relays afferent and efferent vagal transmission (Randich and Aicher, 1988). The dorsal medial subnucleus neurons of the NTS filter signals from peripheral cardiovascular receptors, and relay afferent information from the vagus and glossopharyngeal nerves (Zanutto et al., 2010). In addition, the vagus-NTS pathway plays a major role in the regulation of the cardiovascular reflex, and the vast majority of visceral vagal fibers are relayed by the NTS to multiple brain regions (Fu et al., 2012).

We hypothesize that the cardioprotective effect of acupuncture in myocardial ischemia may involve regulation of the autonomic nervous system *via* the hippocampus, through both inhibition of sympathetic activity and excitation of the vagus nerve. Previous studies have shown that myocardial ischemia induces changes in the autonomic nervous system that affect the dynamic balance between the sympathetic system and the vagus nerve (Cui et al., 2016).

Electroacupuncture (EA) improves the symptoms of myocardial ischemia, modulates autonomic nervous system activity, and reverses the effect of myocardial ischemia on the hippocampal CA1 region (Wu et al., 2015). However, the pathways involved in alleviating myocardial ischemic damage are unclear.

In the present study, we used multi-channel electrophysiological recordings *in vivo* to examine NTS neuronal activity, and at the same time, we observed the vagus nerve and the hemodynamic index, in an effort to clarify how the hippocampus-NTS-vagus nerve pathway provides cardioprotection.

Materials and Methods

Animals

Fifty male Sprague-Dawley rats, 8 weeks of age and weighing 250–300 g, were supplied by the Feeding Center at Anhui Medical University of China (license No. SCXK (Wan) 2011-002). Rats were housed in separate cages (Kangwei IR60) with an independent air supply system for 1 week at 24 ± 2°C and 65% relative humidity under natural lighting. All rats were allowed free access to food and water. All animal procedures were conducted in accordance with the Animal Use Guidelines of Anhui University of Chinese Medicine and Anhui Laboratory Animal Center. The study was approved by the Animal Ethics Committee of Anhui University of Chinese Medicine of China (approval No. 201604-001).

Production of the AMI animal model

Six rats were randomly allocated to the sham group. In the sham group, only punctures were made, and the left anterior descending branch of the coronary artery was not ligated. The remaining 44 rats were used for the AMI model by ligating the left anterior descending branch of the coronary artery (Klocke et al., 2007). High T-wave and J-point elevation (≥ 0.1 mV) on electrocardiogram (ECG) indicated successful generation of the AMI model. Of these 44 animals, 30 met the criteria for AMI, while the remaining 14 died or did not satisfy the criteria. The 30 AMI model rats were randomly divided into the AMI group, AMI + EA group, and the AMI + EA + Lesion group (n = 10 per group).

Lesioning of the hippocampal CA1 region

Three days before artery ligation, the hippocampal CA1 region was lesioned using a previously described method (Wu et al., 2015). Briefly, kainic acid, 1 mg/L, (Sigma-Aldrich, St. Louis, MO, USA) was injected into the hippocampal CA1 region bilaterally at bregma −4.16 mm, lateral 2.8 mm, depth 2.8–3.0 mm, according to the rat brain atlas (Paxinos and Watson, 2009) (**Additional Figure 1A, B**). Three days after surgery, neuronal death was evident in the hippocampal CA1 region (**Additional Figure 2A–D**).

The electrode array (diameter: 35 μm; Plexon Inc., Hong Kong Special Administrative Region, China) was implanted in the NTS and fixed using dental cement. The coordinates according to the rat brain atlas are: bregma −12.72 mm, lateral 0.8–1.6 mm, depth 7.8–8.2 mm (**Additional Figure 1C, D**).

The rat neck surgery mainly involved separation of the arteries and the vagus nerves. Hemodynamic index was recorded during carotid artery cannulation. The discharge of the vagus nerve was recorded using a needle electrode.

All of the experimental indexes (NTS neuronal discharge, ECG, vagus nerve discharge and hemodynamics) were recorded simultaneously (**Additional Figure 2E**).

EA treatment

The *Shenmen* (HT7)-*Tongli* (HT5) segment in the *Shaoyin* heart meridian of the hand was selected with reference to the

human meridian line. The acupuncture positioning criteria of rats were in accordance with *Chinese Veterinary Acupuncture* and previous results (Cui et al., 2016). The *Shenmen* (HT7) acupoint is located on the wrist, at the ulnar end of the crease of the wrist. The *Tongli* (HT5) acupoint is in the radial margin of the flexor carpi ulnaris, 1 inch above the transverse striation of the wrist. For the rats in the AMI + EA group and the AMI + EA + Lesion group, three needles (Φ0.30 × 25 mm) were inserted at the *Shenmen* (HT7)-*Tongli* (HT5) segment with a spacing of 1 mm. The device (Huatuo brand, SDZ-IV type) was purchased from Suzhou Medical Products Co., Ltd., Suzhou, China. The EA parameters were as follows: continuous wave; current of 1 mA; frequency of 2 Hz; duration of 30 minutes, once a day. The EA therapy was started 1 day after AMI, and was performed for three consecutive days in the AMI + EA group and AMI + EA + Lesion group. Rats in the AMI and sham groups received sham stimulation with the instrument switched off.

2,3,5-Triphenyltetrazolium chloride (TTC) staining

The rats were killed by intraperitoneal overdose injection of chloral hydrate. The hearts were taken out and quick-frozen at −20°C for 20 minutes. The hearts were then sliced into six sections and soaked in 2% TTC solution (Servicebio, Wuhan, China) in the dark in a 37°C incubator for 15–30 minutes. The sections were then fixed with paraformaldehyde, and photographed. The area of myocardial infarction was calculated using Image Pro Plus 6.0 software (Media Cybernetics, Silver Spring, MD, USA) (**Figure 1A**).

Peripheral vagus nerve discharge recording

All rats were anesthetized with 10% chloral hydrate (3.5 mL/kg; Sinopharm Chemical Reagent Co., Ltd., St. Louis, MO, USA) by intraperitoneal injection. The room temperature was controlled at 26 ± 2°C, and the rat was placed on a heating pad (Chengdu Taimeng Software Co., Ltd., Chengdu, China) maintained at 36 ± 1°C. The cervical vagus nerve was dissociated, and hooked with a bipolar platinum recording electrode. The reference electrode was inserted into the subcutaneous tissue. The ground electrode was connected to the lower limb. Recording parameters were set, and the discharge frequency of the vagus nerve was recorded by the BIOPAC multi-channel physiological recorder (BIOPAC Systems Inc., St. Louis, MO, USA). Afterwards, fast Fourier transformation filtering was performed on the recorded signals offline. The neural signals were recorded to determine the discharge frequency 5 minutes after EA.

Recording of neuronal discharge in the central nucleus

All rats were anesthetized with 10% chloral hydrate (3.5 mL/kg) by intraperitoneal injection and then fixed on the brain stereotactic apparatus (Stoelting Co., Ltd., St. Louis, MO, USA). The NTS coordinates were according to the rat brain atlas (Paxinos and Watson, 2009). Craniotomy was performed, and an 8-channel microelectrode array was electronically moved to the target nucleus at 5 μm/s. When satisfactory discharge activity was observed, the stable neuronal discharge was recorded for 5 minutes. After the signals were filtered and processed, the selected neuronal discharge signals were subjected to cluster analysis with the Offline Sorter (version 3.3.5, Plexon Inc., Dallas, TX, USA). NeuroExplorer (version 4.13, Nex Technologies, Lexington, MA, USA) was used to analyze the waveform, frequency, characteristics of neuronal discharge, and correlation with the field potential.

Hemodynamics and ECG recording

All rats were anesthetized with 10% chloral hydrate (3.5 mL/kg) by intraperitoneal injection and secured on a heating pad (maintained at 36–37°C) in the supine position. Using conventional standard II lead ECG, the electrodes were inserted into the subcutaneous tissue of the right upper limb and left lower limb. The BIOPAC multi-channel physiological recorder (BIOPAC Systems Inc.) was used to continuously observe respiratory activity, arterial blood pressure, and ECG waveform. After the rats achieved a stable status, the heart rate (HR), mean arterial pressure (MAP) and rate-pressure product (RPP) values were recorded and analyzed with Acknowledge 4.1 (BIOPAC Systems Inc.).

Statistical analysis

Data are expressed as the mean ± SD. Statistical analysis was performed using SPSS 19.0 software (IBM SPSS, Inc., St. Louis, MO, USA). The difference between groups was analyzed by one-way analysis of variance. Test for homogeneity of variance was performed before the comparisons were made between groups. The least significant difference test was used for homogeneity of variance and Tamhane's T2 test was used for heterogeneity of variance.

Cluster analysis, interspike-interval analysis and autocorrelation analysis were used to distinguish and analyze the pattern of NTS neuronal discharge. The pyramidal neurons and interneurons were distinguished based on their characteristic discharge activity. The characteristics of pyramidal neurons were as follows: (1) low mean discharge frequency (0.5–10 Hz) and irregular discharge pattern; (2) histogram showing that a short interspike interval (3–10 ms) is dominant, with exponential attenuation; (3) wide waveform (> 300 μs). The characteristics of interneurons were as follows: (1) high mean discharge frequency (> 5 Hz); (2) interspike interval histogram showing delayed spikes and slow attenuation; (3) narrow waveform (< 250 μs) (Pang and Zhang, 2014).

Real-time spectrum analysis was used to observe local field potential changes. HR, MAP, RPP, vagus nerve discharge, and NTS and interneuronal spike counts were analyzed by linear correlation analysis. The correlation coefficient (R) was calculated. Linear regression was performed using the following model: $y = a + bx$.

Results

Hippocampal regulation by EA at the heart meridian effectively reduced myocardial infarction and ischemic damage

Three days after the EA treatment, the left ventricular infarction areas were calculated in the AMI, AMI + EA and AMI

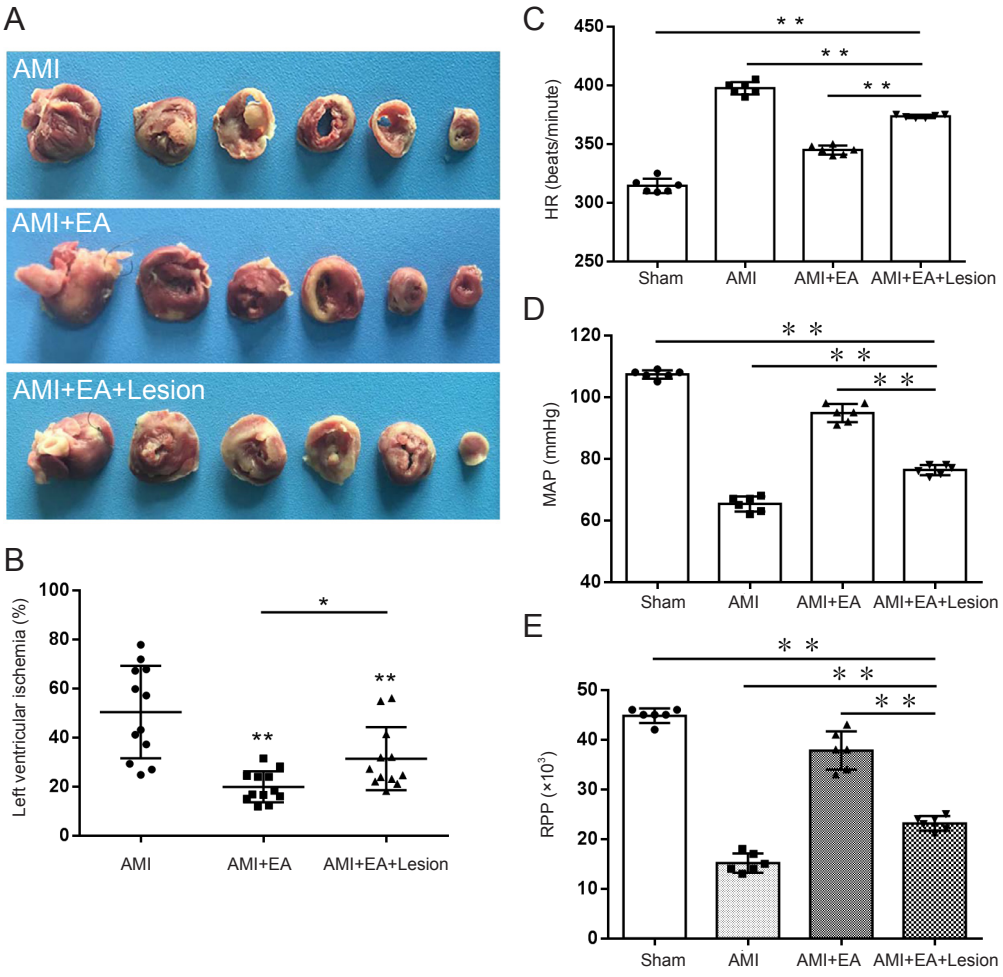

Figure 1 Effect of EA and CA1 lesioning on myocardial infarction area, hemodynamic parameters and vagus nerve discharge activity in AMI rats.
(A) TTC staining of myocardial infarction area; (B) Left ventricular ischemic area; (C) HR; (D) MAP; (E) RPP. The data are expressed as the mean ± SD (n = 6; one-way analysis of variance followed by the least significant difference test). $*P < 0.05$, $**P < 0.01$. EA: electroacupuncture; AMI: acute myocardial ischemia; TTC: 2,3,5-triphenyltetrazolium chloride; HR: heart rate; MAP: mean arterial pressure; RPP: rate-pressure product.

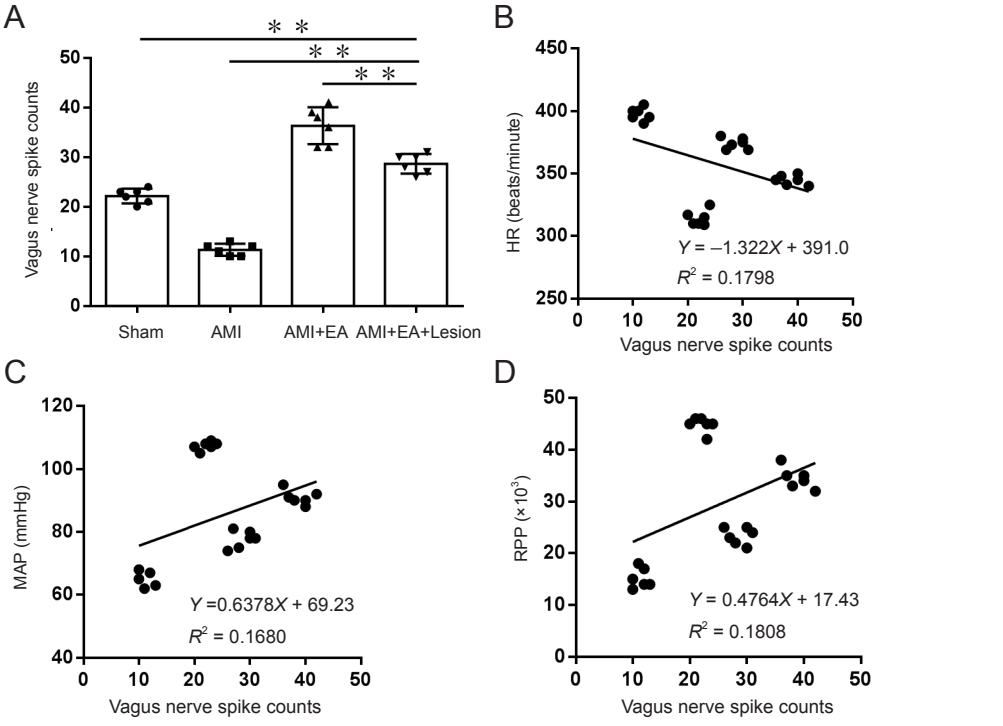

Figure 2 Effect of EA and CA1 lesioning on the discharge frequency of the vagus nerve in AMI rats.
(A) Stable discharge signal of the vagus nerve measured for 5 minutes was recorded immediately (0 minute) after the last EA session for all experimental groups. The data are expressed as the mean ± SD (n = 6; one-way analysis of variance followed by the least significant difference test). $**P < 0.01$. (B–D) Discharge frequency of the vagus nerve was negatively correlated with the HR ($P < 0.05$, $r = -0.424$), but positively correlated with the MAP and RPP ($P < 0.05$, $r = 0.40987$; $P < 0.05$, $r = 0.4252$). EA: Electroacupuncture; AMI: acute myocardial ischemia; HR: heart rate; MAP: mean arterial pressure; RPP: rate-pressure product.

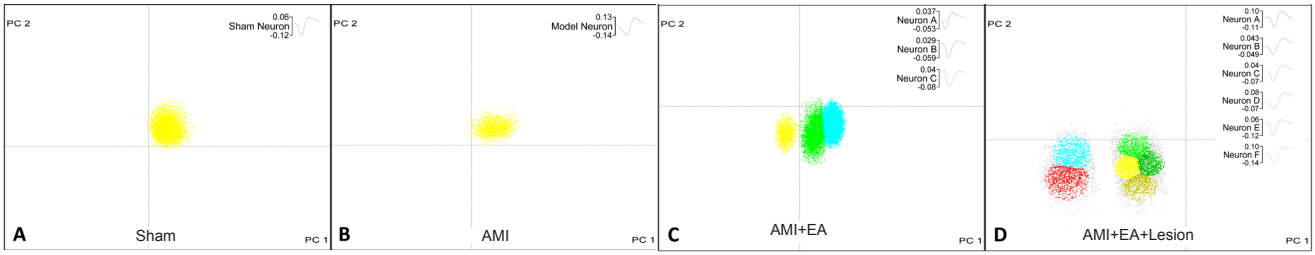

Figure 3 Cluster analysis of the discharge frequency of NTS neurons in AMI rats undergoing EA and CA1 lesioning.
(A–D) There was one pattern of NTS neuronal discharge in the sham group (A), one pattern of discharge in the AMI group (B), three patterns of neuronal discharge in the AMI + EA group (C), and six patterns of neuronal discharge in the AMI + EA + Lesion group (D). Blue, red, light green, dark green and yellow: interneurons; brown: pyramidal cells. EA: electroacupuncture; AMI: acute myocardial ischemia; NTS: nucleus tractus solitarius.

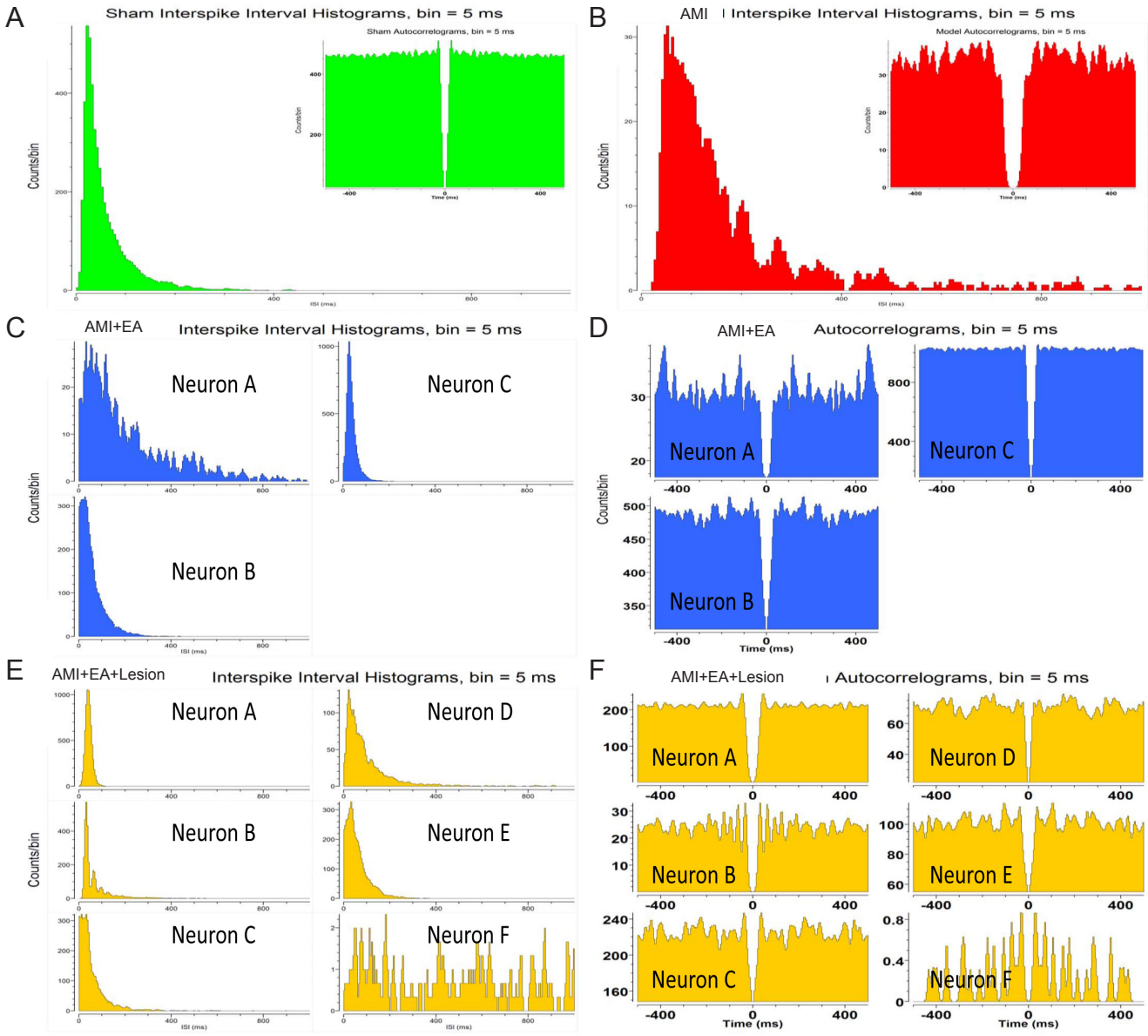

Figure 4 Distinguishing the activity patterns of NTS neurons by autocorrelation analysis and interspike-interval analysis in AMI rats undergoing EA and CA1 lesion.
(A) One interneuron unit's maximum discharge was within 400 ms in the sham group. (B) One interneuron unit's discharge was distributed over a period of 1000 ms, and the maximum discharge was within 400 ms in the AMI group. (C, D) Three interneuron unit discharges were distributed within a period of 1000 ms. The maximum discharge was within 800 ms in Neuron A, within 300 ms in Neuron B, and within 200 ms in Neuron C in the AMI + EA group. (E, F) Five interneuron unit discharges and one pyramidal cell unit discharge. The discharge of Neuron A was distributed within 100 ms. The discharge of Neuron B was distributed within 300 ms, and the maximum was within 200 ms. The discharge of Neuron C was distributed within 200 ms. The discharge of Neuron D was distributed within 400 ms. The discharge of Neuron E was distributed within 300 ms. The discharge of Neuron F was distributed within 1000 ms. The magnitude of the discharge varied in the AMI + EA + Lesion group. EA: Electroacupuncture; AMI: acute myocardial ischemia; NTS: nucleus tractus solitarius.

+ EA + Lesion groups. Compared with the AMI group, the area of myocardial infarction was significantly reduced in the AMI + EA and AMI + EA + Lesion groups ($P < 0.01$). Compared with the AMI + EA group, the area of myocardial infarction was significantly increased in the AMI + EA + Lesion group ($P < 0.05$; **Figure 1B**).

HR, MAP and RPP were recorded after 3 days of EA. Compared with the sham group, HR was significantly higher ($P < 0.01$), but the MAP and RPP were significantly lower ($P < 0.01$), in the AMI group. Compared with the AMI group, HR was significantly lower ($P < 0.01$), but the MAP and RPP were significantly higher ($P < 0.01$), in the AMI + EA group. Compared with the AMI + EA group, HR was significantly higher ($P < 0.01$), but the MAP and RPP were significantly lower ($P < 0.01$), in the AMI + EA + Lesion group (**Figure 1C–E**).

EA of the heart meridian affected hippocampal regulation of vagus nerve discharge

The stable discharge activity of the vagus nerve for a period of 5 minutes was recorded immediately (0 minutes) after the last EA session. Discharge frequency of the vagus nerve was significantly lower in the AMI group compared with the sham group ($P < 0.01$). Compared with the AMI group, discharge frequency of the vagus nerve was significantly higher in the AMI + EA group ($P < 0.01$). Discharge frequency of the vagus nerve was significantly lower in the AMI + EA + Lesion group compared with the AMI + EA group ($P < 0.01$; **Figure 2A**).

Correlation analysis was performed for discharge frequency of the vagus nerve and hemodynamic indexes. The discharge frequency of the vagus nerve was negatively correlated with the HR ($P < 0.05$, $r = -0.424$), but positively correlated with the MAP and RPP ($P < 0.05$, $r = 0.40987$; $P < 0.05$, $r = 0.4252$) (**Figures 2B–D**). These results suggest that EA at the heart meridian modulates the hippocampal regulation of vagal discharge activity to reduce myocardial ischemic injury.

EA of the heart meridian impacted the hippocampal regulation of NTS neurons

Multi-channel *in vivo* recording electrodes were used to record stable discharge by the NTS for 5 minutes immediately (0 minute) after the last EA session. Data processing was used to obtain the discharge time sequence of single neurons and clusters of neurons in each group (**Figure 3** and **Additional Figure 3**). We identified one pattern of neuronal activity in the sham and AMI groups, three patterns in the AMI + EA group, and six patterns in the AMI + EA + Lesion group. Interspike interval analysis and autocorrelation analysis were performed to distinguish the firing types. In the AMI group, one interneuron unit discharge was distributed over a period of 1000 ms, and the maximum discharge was within 400 ms. In the AMI + EA group, three interneuron unit discharges were distributed over 1000 ms, and the maximum discharge was within 800 ms in Neuron A, within 300 ms in Neuron B, and within 200 ms in Neuron C. In the AMI + EA + Lesion group, five interneuron unit discharges and one pyramidal cell unit discharge were recorded. The discharge of Neuron A was distributed over a period of 100 ms; the discharge of Neuron B was distributed over 300 ms, with a maximum within 200 ms; the discharge of Neuron C was distributed over 200 ms; the discharge of Neuron D was distributed over 400 ms; the discharge of Neuron E was distributed over 300 ms; and the discharge of Neuron F was distributed over 1000 ms. The discharge patterns differed (**Figure 4**).

The discharge time sequence (time = 300 seconds) of each group of neurons was converted to a histogram of discharge frequency. In the sham group, the total discharge frequency of the NTS neurons was 5010 ± 58.89 Hz for the interneurons. In the AMI group, the total discharge frequency of the NTS neurons was 931.67 ± 14.38 Hz, all of which were interneurons. In the AMI + EA group, the total discharge frequency was 14,195 ± 240.51 Hz in the NTS interneurons, 1322 ± 23.37 Hz in Neuron A, 5175 ± 18.34 Hz in Neuron B, and 7716 ± 29.53 Hz in Neuron C. In the AMI + EA + Lesion group, the total discharge frequency of the NTS neurons was 23,105 ± 174.59 Hz. The values were 6984 ± 43.26 Hz, 3778 ± 53.74 Hz, 4751 ± 18.26 Hz, 2372 ± 32.13 Hz and 5014 ± 25.67 Hz for the interneurons, and 259 ± 3.28 Hz for the pyramidal cells. The total discharge frequency of NTS neurons and the discharge frequency of the interneurons were significantly different between groups ($P < 0.01$; **Figure 5A, B**).

Real-time spectrum analysis was used to investigate the changes in spectral characteristics over time. The intensities of the spectral energy of the local field potential for the four groups were in the following order: AMI + EA + Lesion group > sham group > AMI + EA group > AMI group. These findings suggest that the hippocampus is involved in mediating the cardioprotective effect of EA at the heart meridian by regulating the spectral energy of the NTS (**Additional Figure 4**).

NTS neuronal activity correlated with vagal discharge and hemodynamics following EA of the heart meridian

A correlation analysis was performed of the total discharge frequency of NTS neurons, the discharge frequency of the vagus nerve and hemodynamic parameters. The total discharge frequency of NTS neurons was positively correlated with the discharge frequency of the vagus nerve ($P < 0.01$, $r = 0.7021$), but not with HR ($P > 0.05$, $r = 0.01439$), MAP ($P > 0.05$, $r = -0.08993$) or RPP ($P > 0.05$, $r = -0.03263$) (**Figure 6**).

Correlation analysis was conducted for the AMI + EA and AMI + EA + Lesion groups. This analysis showed that of the three types of neurons in the AMI + EA group, only one neuron (neuron C) was negatively correlated with the discharge frequency of the vagus nerve ($P < 0.05$, $r = -0.87749$), the HR ($P < 0.01$, $r = -0.91902$), the MAP ($P < 0.05$, $r = -0.85691$), and the RPP ($P < 0.01$, $r = -0.91902$) (**Figure 7**). Among the six types of neurons in the AMI + EA + Lesion group, three correlated with vagal discharge and hemodynamic indexes. Neuron C was positively correlated with vagal discharge frequency ($P < 0.01$, $r = 0.8905$), HR ($P < 0.01$, $r = 0.9347$), MAP ($P < 0.05$, $r = 0.8474$) and RPP ($P < 0.05$, $r = 0.8637$). Neuron D was positively correlated with the discharge frequency of the vagus nerve ($P < 0.01$, $r = 0.9725$), HR ($P < 0.01$, $r = 0.9089$), MAP ($P < 0.01$, $r = 0.9691$) and RPP ($P < 0.01$, $r = 0.9407$). Neuron E was positively correlat-

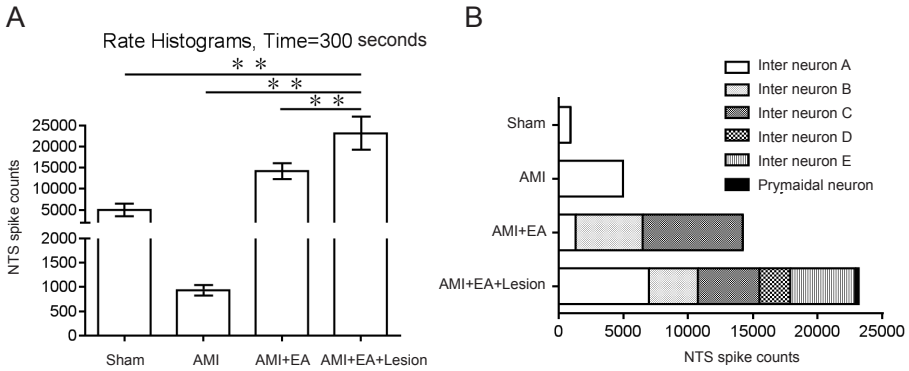

Figure 5 Discharge frequency of the NTS and classification of the neurons in AMI rats undergoing EA and CA1 lesioning.
(A) Discharge frequency of NTS neurons in each group. The data are expressed as the mean ± SD (n = 6; one-way analysis of variance followed by the least significant difference test). **P < 0.01. (B) Classification of the interneur ons and pyramidal cells. EA: Electroacupuncture; AMI: acute myocardial ischemia; NTS: nucleus tractus solitarius.

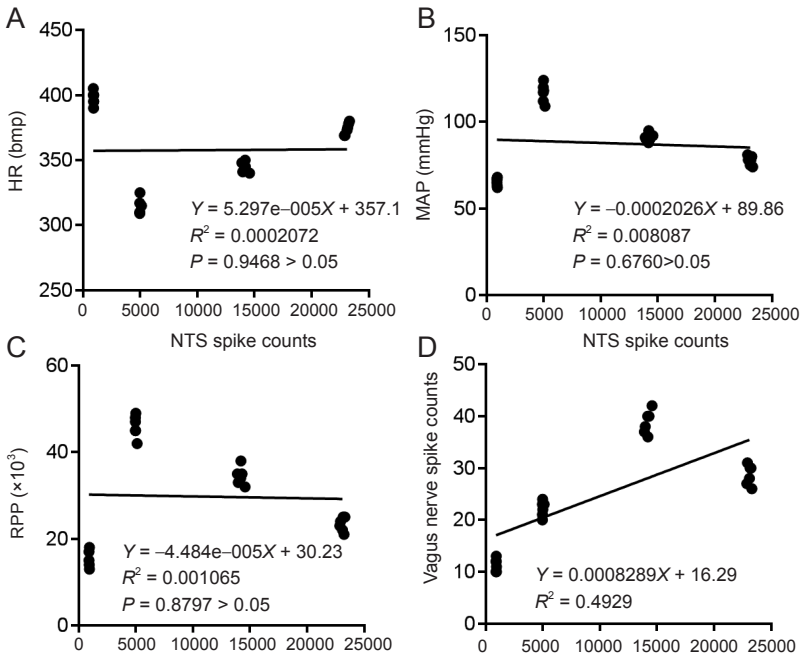

Figure 6 Correlation analysis of the total discharge frequency of NTS neurons and the total discharge frequency of the vagus nerve and hemodynamic parameters.
(A) Total discharge frequency of the NTS neuron is not correlated with the HR (P > 0.05, r = 0.01439). (B) Total discharge frequency of the NTS neuron is not correlated with the MAP (P > 0.05, r = –0.08993). (C) Total discharge frequency of the NTS neuron is not correlated with the RPP (P > 0.05, r = –0.03263). (D) Total discharge frequency of the NTS neuron is correlated with the discharge frequency of the vagus nerve (P < 0.01, r = 0.7021). NTS: Nucleus tractus solitarius; HR: heart rate; MAP: mean arterial pressure; RPP: rate-pressure product.

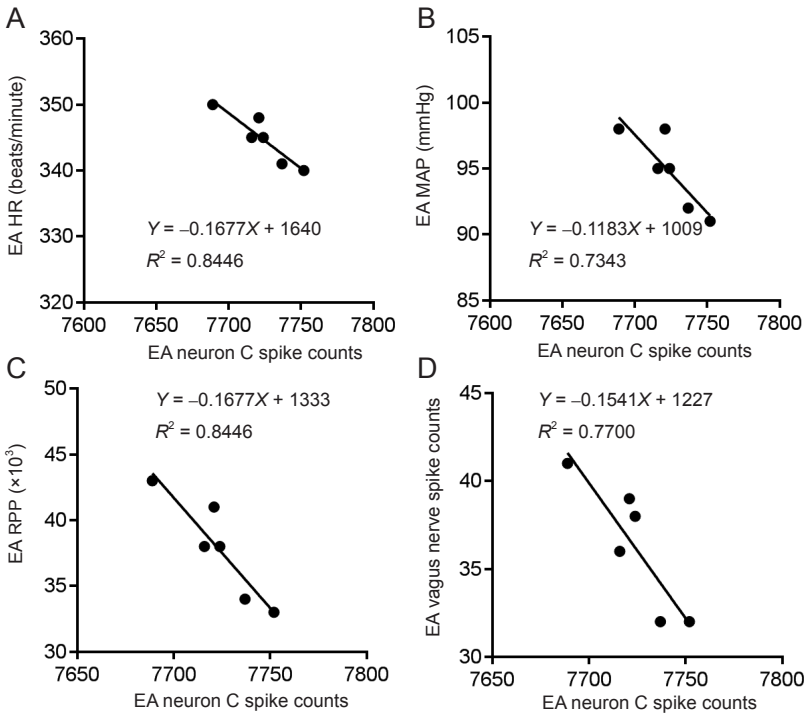

Figure 7 Correlation analysis of the discharge frequency of neuron C, the total discharge frequency of the vagus nerve, and hemodynamic parameters in the AMI + EA group.
(A–D) The only one pattern of interneuronal firing (interneuron C) was negatively correlated with the discharge frequency of the vagus nerve (P < 0.05, r = –0.87749), the HR (P < 0.01, r = –0.91902), the MAP (P < 0.05, r = –0.85691), and the RPP (P < 0.01, r = –0.91902). EA: Electroacupuncture; AMI: acute myocardial ischemia; HR: heart rate; MAP: mean arterial pressure; RPP: rate-pressure product.

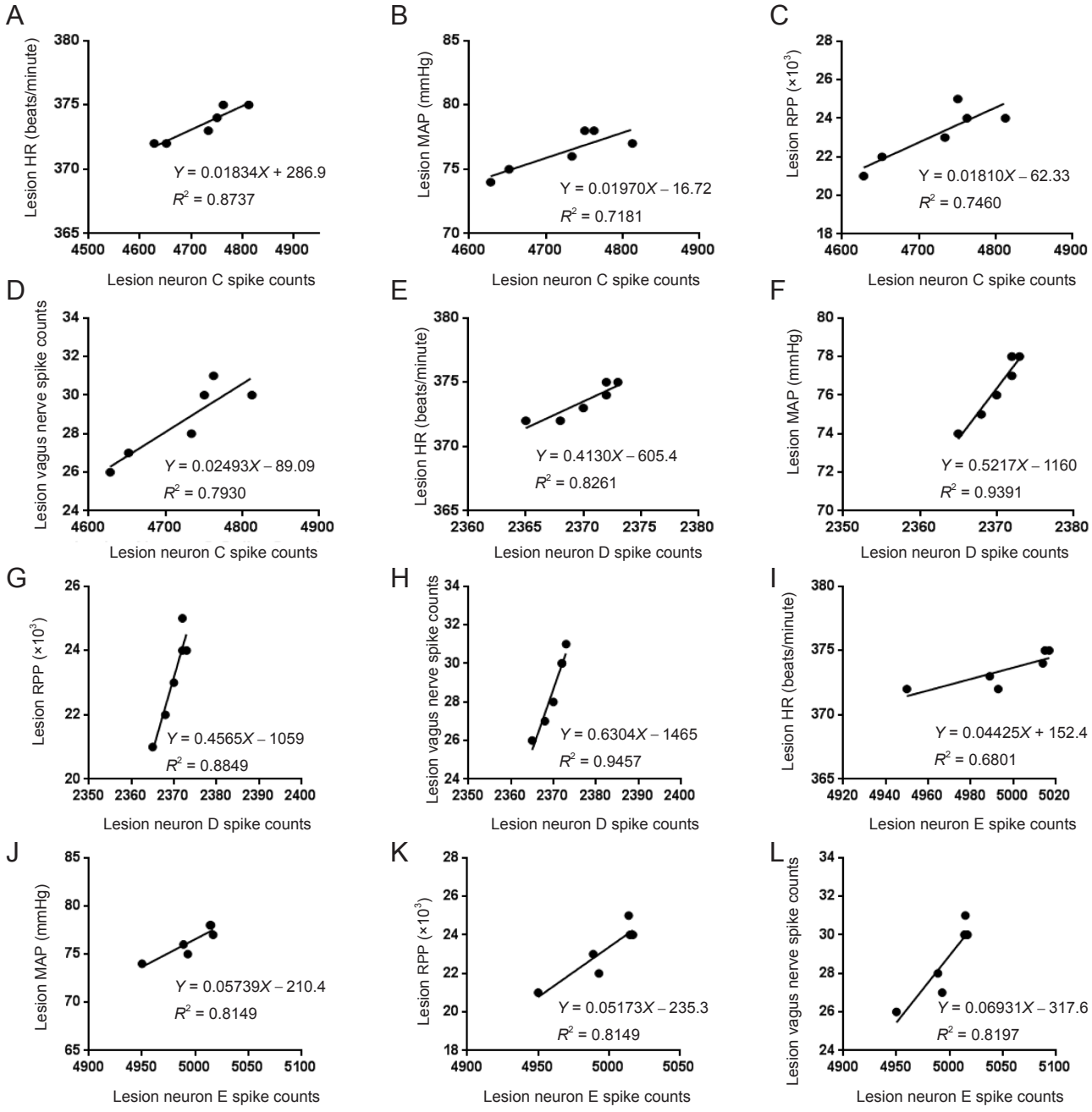

Figure 8 Correlation analysis of the discharge frequency of neuron C, neuron D and neuron E, the total discharge frequency of the vagus nerve, and hemodynamic parameters in the AMI + EA + Lesion group.

(A–D) Of the six types of neurons in the AMI + EA + Lesion group, three types of interneurons correlated with vagus nerve discharge and hemodynamic indexes. Interneuron C was positively correlated with vagal discharge frequency ($P < 0.01$, $r = 0.8905$), HR ($P < 0.01$, $r = 0.9347$), MAP ($P < 0.05$, $r = 0.8474$) and RPP ($P < 0.05$, $r = 0.8637$). (E–H) Interneuron D was positively correlated with vagal discharge frequency ($P < 0.01$, $r = 0.9725$), HR ($P < 0.01$, $r = 0.9089$), MAP ($P < 0.01$, $r = 0.9691$) and RPP ($P < 0.01$, $r = 0.9407$). (I–L) Interneuron E was positively correlated with vagal discharge frequency ($P < 0.01$, $r = 0.9054$), HR ($P < 0.05$, $r = 0.8247$), MAP ($P < 0.01$, $r = 0.9027$) and RPP ($P < 0.01$, $r = 0.9027$). EA: Electroacupuncture; AMI: acute myocardial ischemia; HR: heart rate; MAP: mean arterial pressure; RPP: rate-pressure product.

ed with the discharge frequency of the vagus nerve ($P < 0.01$, $r = 0.9054$), HR ($P < 0.05$, $r = 0.8247$), MAP ($P < 0.01$, $r = 0.9027$) and RPP ($P < 0.01$, $r = 0.9027$) (**Figure 8**).

Discussion

The association between the meridian-viscera and the brain was the theoretical basis of acupuncture treatment for AMI

Research on the links between the meridians, viscera and the brain is a hot topic in systems biomedicine. Systems theory and Chinese medicine are combined, emphasizing that biological phenomena should be studied and grasped from the systemic and holistic levels. The study of the association between the meridians and viscera are combined with modern neuroscience to investigate the connection between the meridian-viscera and the brain, especially the limbic-hypothalamic-autonomic axis (Zhou et al., 2008).

Acupuncture alleviates myocardial ischemic tissue damage by regulating the central nervous system, cardiovascular activity, myocardial tissues and the antioxidant system (He et al., 2014). EA at heart acupoints has been shown to regulate hypoxia-inducible factor-1α protein, downregulate ASIC2 and ASIC3 gene expression in ischemic myocardial tissue, effectively alleviate damage to myocardial cells, and reduce the area of myocardial infarction (Wang et al., 2015; Ding et al., 2017). Furthermore, it upregulates heat shock protein 27 and heat shock protein 70 expression in heart tissue to protect against myocardial ischemic damage (Sakamoto et al., 2000; Tan et al., 2017). A large number of studies have shown that EA inhibits expression of the pro-apoptotic gene Bax and upregulates the anti-apoptotic gene Bcl-2 to reduce apoptosis in myocardial tissue (Zhang et al., 2009). Furthermore, EA downregulates CLCa and inhibits PKC activation to inhibit AQP 1 protein expression, thereby exerting cardioprotection (Bai et al., 2015; Cheng et al., 2016; Cai et al., 2017). EA at the heart meridian has been shown to modulate gene expression in the hypothalamus, including that of the Trh and Crh genes. This may be involved in the protective effects of EA at the heart meridian and small intestine meridian (Zhou et al., 2007).

Our current findings suggest that the total discharge frequency of the NTS is correlated with the discharge of the vagus nerve. Furthermore, some, but not all, NTS neurons were correlated with hemodynamic indexes. Therefore, we speculate that some interneurons in the NTS mediate the cardioprotective effects of EA at the heart meridian.

The limbic-hypothalamic-autonomic axis was the neural substrate targeted by EA to alleviate heart disease

The hippocampus is a limbic forebrain structure. Not only is the hippocampus an important center for regulating memory and cognition, but also an important center for regulating cardiovascular function. The hippocampus has complex connections with the paraventricular nucleus, NTS, amygdala, locus coeruleus and medial prefrontal cortex (Chiba, 2000; Castle et al., 2005; Vertes et al., 2007; Mello-Carpes and Izquierdo, 2013; Zhang and Hernandez, 2013). A recent study showed that the cognitive dysfunction induced by myocardial ischemia in adult mice is associated with reactive gliosis in the hippocampus and a decrease in neurogenesis (Evonuk et al., 2017).

The NTS is a relay station for visceral primary afferent fibers, and has connections with many nuclei and regions in the brain. Xiao et al. (2000) found that NTS fibers project to the central amygdala via the lateral parabrachial nucleus. This pathway might play a major role in regulating cardiovascular activity. The NTS projects onto catecholaminergic cells in the bed nucleus of the stria terminalis, preoptic area, central amygdala, locus coeruleus and spinal cord, which may also be involved in regulating the cardiovascular and sympathetic nervous systems (Sim and Joseph, 1994).

Our results show that the hippocampus modulates NTS neuronal activity in rats with myocardial ischemia. Damage to the hippocampal CA1 region increased neuronal activity and the types of neuronal firing in the NTS. The NTS receives sensory signals from the heart after ischemia as well as instructions from higher centers to regulate the cardiovascular system. This may explain why different neuronal discharge patterns were recorded in the NTS.

Multi-channel recording *in vivo* allowed study of central neuronal activity

Multi-channel recording *in vivo* is an extracellular recording technique that allows measurement of the extracellular field potential at the electrode tip (Buzsaki et al., 2012). Filtering technology can help distinguish neural activity from different sources. One type of signal is the multiple-unit activity recorded around the electrode with the 300–400 Hz high-pass filter. The other type of signal is the local field potential activity obtained with the 300 Hz low-pass filter (Jansen and Ter Maat, 1992; Gray et al., 1995; Csicsvari et al., 1999). This method can synchronously record the electrical activity of a large number of neurons in multiple brain regions. This is useful for the study of individuals receiving a specific stimulus (*e.g.*, EA) or performing a specific behavioral task. The method can help clarify the spatiotemporal relationship between neuronal discharges in different brain regions. Brain coding mechanisms for external events can be studied by analyzing neuronal firing patterns (Wang et al., 2003).

Summary

The NTS is a complex mixed sensory/motor nerve relay nucleus. The NTS receives afferent sensory input from the inferior vagal nerve and provides efferent signals to higher brain centers (*e.g.*, the hippocampus) to regulate cardiovascular activity. Therefore, EA at the heart meridian likely alleviates myocardial ischemic injury *via* the hippocampus-NTS-vagus nerve pathway. During EA stimulation at *Shenmen* (HT7)-*Tongli* (HT5), the acupuncture signals are conveyed to the central nervous system *via* the peripheral nerves. Signal processing occurs in the hippocampus, and the output from this structure then regulates the excitability of specific neurons in the NTS. Subsequently, signals from the NTS are transmitted to the vagus nerve to regulate cardiac activities and provide cardioprotection.

Conclusion

Although we identified the types of neurons involved in the cardioprotective action of EA based on discharge patterns, we did not analyze the relationship between the neurons. In addition, we did not assess relevant neurotransmitter indicators. Neurons should be associated with neurotransmitters to better identify the neuronal types involved in the protective effect of EA against myocardial ischemia. These unresolved issues will be the focus of our future studies.

Author contributions: *MQZ and YPZ conceived and supervised the study. MQZ, YPZ and SC designed the study. SC, SBW and KW performed experiments. SC designed new electrode and tools, and analyzed data. SC and MQZ wrote the paper. SC, GQZ and MQZ made paper revisions. All authors reviewed the results and approved the final version of the paper.*
Conflicts of interest: *All authors declare no personal or financial conflicts of interest.*
Financial support: *This study was supported by the National Natural Sci-*

ence Foundation of China, No. 81273858; a grant from the Anhui University Research and Innovation Platform Team Construction Project in China, No. 2015TD033. The conception, design, execution, and analysis of experiments, as well as the preparation of and decision to publish this manuscript, were made independent of any funding organization.

Institutional review board statement: *The study protocol was approved by the Animal Ethics Committee of Anhui University of Chinese Medicine in China (approval No. 201604-001). The experimental procedure followed the United States National Institutes of Health Guide for the Care and Use of Laboratory Animal (NIH Publication No. 85-23, revised 1985).*

Copyright license agreement: *The Copyright License Agreement has been signed by all authors before publication.*

Data sharing statement: *Datasets analyzed during the current study are available from the corresponding author on reasonable request.*

Plagiarism check: *Checked twice by iThenticate.*

Peer review: *Externally peer reviewed.*

Additional files:

Additional Figure 1: *Central nucleus coordinate location.*

Additional Figure 2: *Hippocampus CA1 HE staining and experimental flow graph.*

Additional Figure 3: *The rate histograms of neurons in each group.*

Additional Figure 4: *Real-time spectrum analysis of the NTS's local field potential discharge.*

References

Bai ZH, Wu ZL, Su Z, Cong PW, Chen YG, Li CR, Wu L (2015) Effect of Electroacupuncture stimulation of "Neiguan" (PC 6) on expression of myocardial chloride channel-related genes, PKC and PKG proteins in myocardial ischemia rats. Zhen Ci Yan Jiu 40:439-443.

Buzsaki G, Anastassiou CA, Koch C (2012) The origin of extracellular fields and currents--EEG, ECoG, LFP and spikes. Nat Rev Neurosci 13:407-420.

Cai R, Hu L, Shen G, Yu Q, Wang J, Wu Z, Li M (2017) Effects of electroacupuncture preconditioning on expression of aquaporin-1 and activity of protein kinase C in myocardium of rats with acute myocardial ischemia-reperfusion injury. Zhongguo Zhen Jiu 37:157-161.

Castle M, Comoli E, Loewy AD (2005) Autonomic brainstem nuclei are linked to the hippocampus. Neuroscience 134:657-669.

Chen L, Tian HN, Gao YF (2016) Influence of Sheng-Huang mixture on cardiocyte apoptosis and bax and bcl-2 mRNA expression in a rat model of ischemia-reperfusion injury. Zhongguo Zuzhi Gongcheng Yanjiu 20:4049-4054.

Cheng ZD, Chen YG, Li XM, Qin PL, Liang FR, Rong PJ (2016) Effects of electroacupuncture on expression of myocardial chloride channel-2 and CLCA proteins in mice with acute myocardial ischemia. Zhen Ci Yan Jiu 41:423-428.

Chiba T (2000) Collateral projection from the amygdalo--hippocampal transition area and CA1 to the hypothalamus and medial prefrontal cortex in the rat. Neurosci Res 38:373-383.

Csicsvari J, Hirase H, Czurko A, Mamiya A, Buzsaki G (1999) Oscillatory coupling of hippocampal pyramidal cells and interneurons in the behaving Rat. J Neurosci 19:274-287.

Cui S, Xu J, Wang J, Wu SB, Zhou YP, Zhou MQ (2016) Effect of electroacupuncture stimulation of heart meridian on autonomic nervous activities in acute myocardial ischemia rats. Zhen Ci Yan Jiu 41:515-520.

Ding YJ, Lu SF, Chen X, Peng YJ, ZHu BM (2017) Effect of electroacupuncture pretreatment at different time on myocardial ischemia injury and expression of HIF-1α. Nanjing Zhongyiyao Daxue Xuebao 33:40-43.

Evonuk KS, Prabhu SD, Young ME, DeSilva TM (2017) Myocardial ischemia/reperfusion impairs neurogenesis and hippocampal-dependent learning and memory. Brain Behav Immun 61:266-273.

Fu R, Zhao Y, Wang TH (2012) The vagus nerve - nucleus of tract solitary pathways for cardiovascular physiological regulation function. Guangdong Yixue 33:560-563.

Gray CM, Maldonado PE, Wilson M, McNaughton B (1995) Tetrodes markedly improve the reliability and yield of multiple single-unit isolation from multi-unit recordings in cat striate cortex. J Neurosci Methods 63:43-54.

He SY, Lu SF, Zhu BM (2014) Progress of researches on mechanisms of acupuncture therapy underlying improving myocardial ischemia and the future approach for in-depth study on its mechanisms from epigenetics. Zhen Ci Yan Jiu 39:73-78.

Jansen RF, Ter Maat A (1992) Automatic wave form classification of extracellular multineuron recordings. J Neurosci Methods 41:123-132.

Klocke R, Tian W, Kuhlmann MT, Nikol S (2007) Surgical animal models of heart failure related to coronary heart disease. Cardiovasc Res 74:29-38.

Liu ZW, Tang XJ, Zhang T (2007) Progress of hippocampus in the control and regulation of automatic nervous system. Sheng Li Ke Xue Jin Zhan 38:168-171.

Lu ZY, Zhong NS (2009) Internal Medicine. Beijing: People's Medical Publishing House.

Mello-Carpes PB, Izquierdo I (2013) The Nucleus of the Solitary Tract → Nucleus Paragigantocellularis → Locus Coeruleus → CA1 region of dorsal hippocampus pathway is important for consolidation of object recognition memory. Neurobiol Learn Mem 100:56-63.

Pang G, Zhang GL (2014) Subcellular localization of serotonin 2 A receptor in dorsal hippocampal CA1 area and its effect on neuronal firing. Zhongguo Yaoli Xue Tongbao 30:1262-1266.

Paxions G, Watson C (2009) The Rat Brain in Stereotaxic Coordinates, Compact 6th ed. New York: Academic Press.

Randich A, Aicher SA (1988) Medullary substrates mediating antinociception produced by electrical stimulation of the vagus. Brain Res 445:68-76.

Sakamoto K, Urushidani T, Nagao T (2000) Translocation of HSP27 to sarcomere induced by ischemic preconditioning in isolated rat hearts. Biochem Biophys Res Commun 269:137-142.

Sim LJ, Joseph SA (1994) Efferents of the opiocortin-containing region of the commissural nucleus tractus solitarius. Peptides 15:169-174.

Tan CF, Yan J, Wang C, Chang XR, Xie WJ, Yang JJ, Liu M, Lin HB, He XC (2017) Effects of electroacupuncture and moxibustion pretreatment on expressions of HSP 27, HSP 70, HSP 90 at different time-points in rabbits with myocardial ischemia-reperfusion injury. Zhen Ci Yan Jiu 42:31-38.

Vertes RP, Hoover WB, Szigeti-Buck K, Leranth C (2007) Nucleus reuniens of the midline thalamus: link between the medial prefrontal cortex and the hippocampus. Brain Res Bull 71:601-609.

Wang JY, Luo F, Han JS (2003) *in vivo* multi-channel recording methods for central neural activities. Sheng Li Ke Xue Jin Zhan 34:356-358.

Wang SD, Chen YG, Dong BQ, Zhang LD, Rong PJ (2015) Influence of electroacupuncture at Neiguan (PC 6) on expression of HIF-1α and ASICs in rats with myocardial ischemia. Zhonghua Zhongyiyao Zazhi 30:2890-2892.

Wu S, Cao J, Zhang T, Zhou Y, Wang K, Zhu G, Zhou M (2015) Electroacupuncture ameliorates the coronary occlusion related tachycardia and hypotension in acute rat myocardial ischemia model: potential role of hippocampus. Evid Based Complement Alternat Med 2015:925987.

Xiao M, Ding J, Zuo GP (2000) Projections of the nucleus of the solitary tract and the parabrachial nucleus to the central nucleus of the amygdala: an anatomical observation with the technique of horseradish peroxidase tracing in the rat. Nanjing Yike Daxue Xuebao 20:371-373.

Zaman S, Kovoor P (2014) Sudden cardiac death early after myocardial infarction: pathogenesis, risk stratification, and primary prevention. Circulation 129:2426-2435.

Zanutto BS, Valentinuzzi ME, Segura ET (2010) Neural set point for the control of arterial pressure: role of the nucleus tractus solitarius. Biomed Eng Online 9:4.

Zhang H, Liu L, Huang G, Zhou L, Wu W, Zhang T, Huang H (2009) Protective effect of electroacupuncture at the Neiguan point in a rabbit model of myocardial ischemia-reperfusion injury. Can J Cardiol 25:359-363.

Zhang L, Hernandez VS (2013) Synaptic innervation to rat hippocampus by vasopressin-immuno-positive fibres from the hypothalamic supraoptic and paraventricular nuclei. Neuroscience 228:139-162.

Zhou MQ, Zhou YP, Wang KM, Hu L, Shen XM, Wang YL, Chen YN (2007) Study on hypothalamus's gene expression of electroacupuncture at the heart meridian of hand-Shaoyin and the small intestine meridian of hand-Taiyang in intervening acute myocardial ischemia in rats. Anhui Zhongyi Xueyuan Xuebao 26:18-21.

Zhou YP, ZHou MQ, Wang KM, Hu L, Wu ZJ, Wang YL, Chen YN (2008) Research on the correlation between channels,viscera and brain is the breakthrough of theory combination between traditional chinese medicine and western medicine. Anhui Zhongyi Xueyuan Xuebao 27:1-7.

Zhu JC, Ma H, Wang JK (2008) The changes of long term potentiation and expression of TNF-α and IL-1β in rats with acute myocardial ischemic reperfusion injury. Zhongguo Yike Daxue Xuebao 37:124-127.

Zhu JC, Yin H, Tan WF, Li Y (2012) Effects of sevoflurane precondition on NMDA receptors in hippocampus of rats after myocardial ischemia-reperfusion. Zhongguo Yike Daxue Xuebao 41:686-687,695.

(*Copyedited by Patel B, Frenchman B, Yu J, Li CH, Qiu Y, Song LP, Zhao M*)

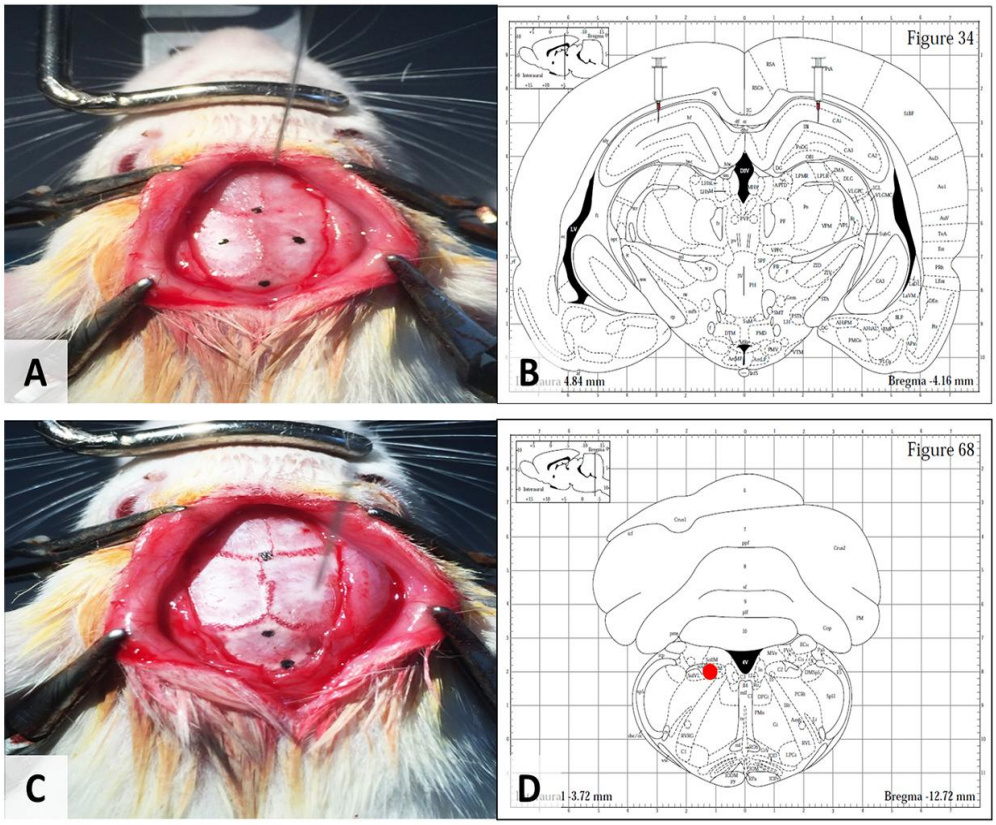

Additional Figure 1 Central nucleus coordinate location.

(A, B) Coordinates of lesion bilateral hippocampal CA1 area. (C, D) The coordinates of NTS.

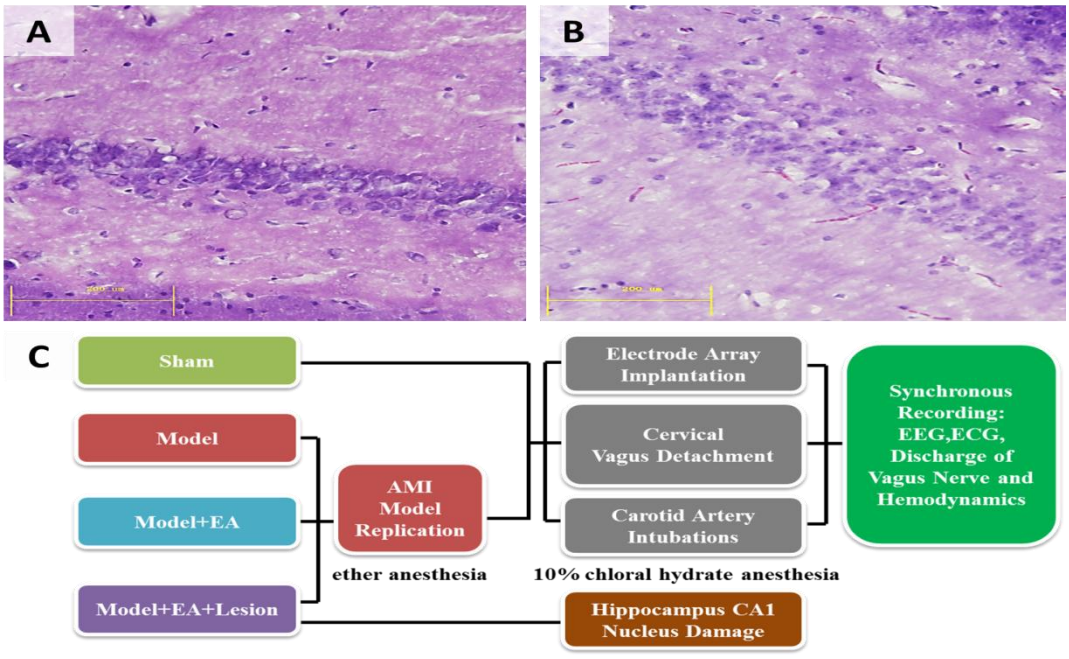

Additional Figure 2 Hippocampus CA 1 HE staining and experimental flow graph.

(A, B) Changes of lesion bilateral hippocampal CA1 area (HE staining). Scale Bars: 200 μ m. (C) The flow diagram of experiment.

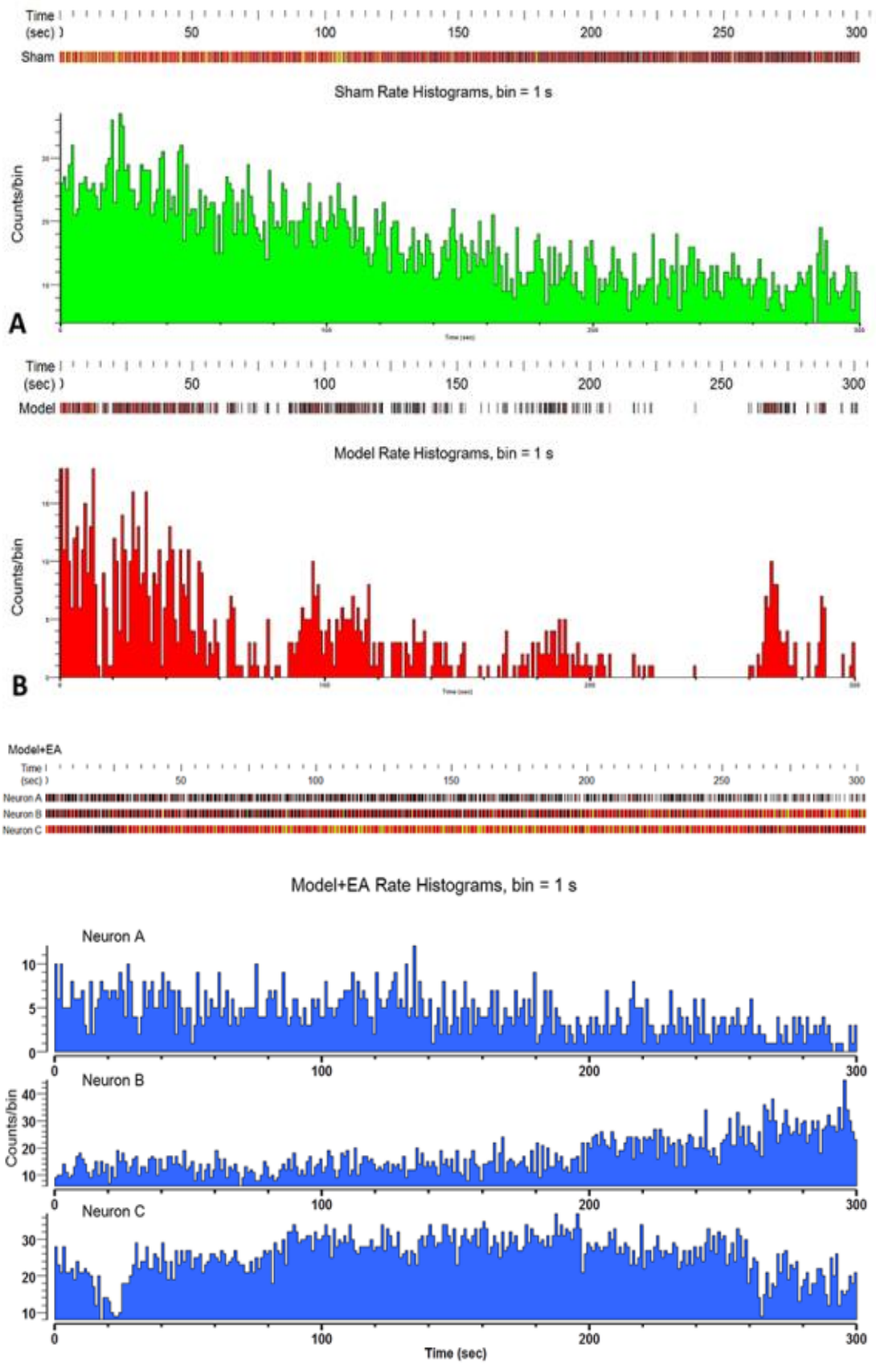
Time (sec)
50
100
150
200
250
300
Sham
Sham Rate Histograms, bin = 1 s
Counts/bin
A
Time (sec)
Model
Model Rate Histograms, bin = 1 s
B
Model+EA
Neuron A
Neuron B
Neuron C
Model+EA Rate Histograms, bin = 1 s
Time (sec)

C

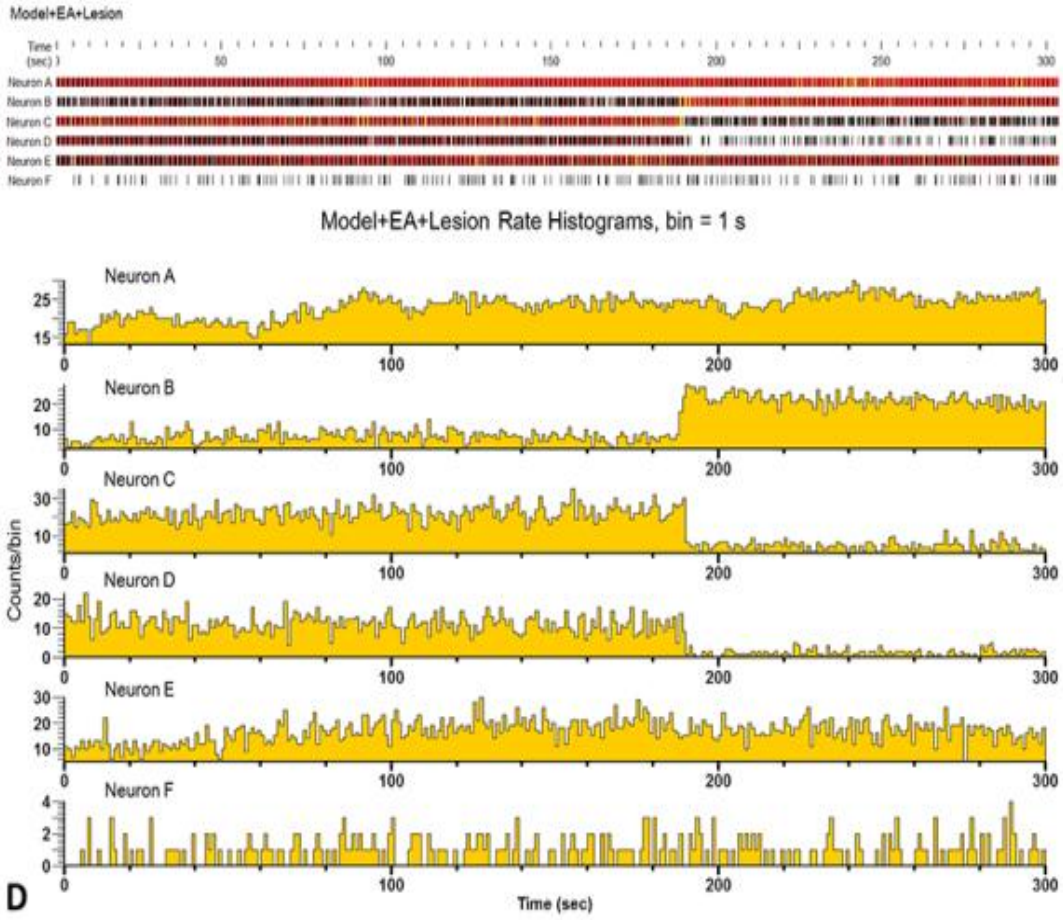

Additional Figure 3 The rate histograms of neurons in each group.

(A-D) the frequency of NTS's neurons and max peak of NTS in each group with the time series (time = 300 s);(A) The sham group has one neuron; (B) AMI group has one neuron and the frequency is lower than the sham group; (C) AMI +EA group has three neurons, the neuron A and neuron B effect each other; (D) AMI +EA+Lesion group has six neurons, the neuron B, C and D effect each other.

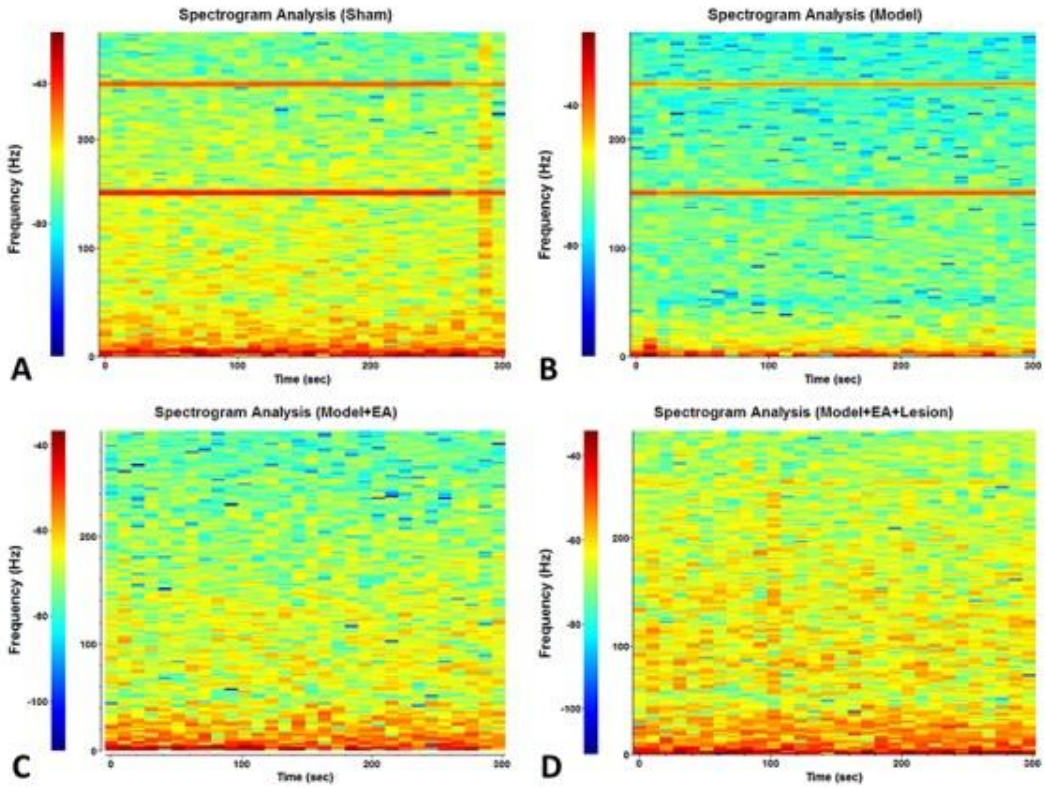

Additional Figure 4. Real-time spectrum analysis the NTS's LFP discharge.

According to the intensity of the spectral energy of the local field potential (LFP), the 4 groups were sequenced as follows: (D) AMI + EA + Lesion group > (A) the Sham group > (C) e AMI + EA group > (B) AMI group.